

# K<sub>2P</sub> channels in plants and animals

Wendy González • Braulio Valdebenito • Julio Caballero • Gonzalo Riadi •  
Janin Riedelsberger • Gonzalo Martínez • David Ramírez • Leandro Zúñiga •  
Francisco V. Sepúlveda • Ingo Dreyer • Michael Janta • Dirk Becker

**Abstract** Two-pore domain potassium (K<sub>2P</sub>) channels are membrane proteins widely identified in mammals, plants, and other organisms. A functional channel is a dimer with each subunit comprising two pore-forming loops and four transmembrane domains. The genome of the model plant *Arabidopsis thaliana* harbors five genes coding for K<sub>2P</sub> channels. Homologs of *Arabidopsis* K<sub>2P</sub> channels have been found in all higher plants sequenced so far. As with the K<sub>2P</sub> channels in mammals, plant K<sub>2P</sub> channels are targets of external and internal stimuli, which fine-tune the electrical properties of the membrane for specialized transport and/or signaling tasks. Plant K<sub>2P</sub> channels are modulated by signaling molecules such as intracellular H<sup>+</sup> and calcium and physical factors like temperature and pressure. In this review, we ask the following:

What are the similarities and differences between K<sub>2P</sub> channels in plants and animals in terms of their physiology? What is the nature of the last common ancestor (LCA) of these two groups of proteins? To answer these questions, we present physiological, structural, and phylogenetic evidence that discards the hypothesis proposing that the duplication and fusion that gave rise to the K<sub>2P</sub> channels occurred in a prokaryote LCA. Conversely, we argue that the K<sub>2P</sub> LCA was most likely a eukaryote organism. Consideration of plant and animal K<sub>2P</sub> channels in the same study is novel and likely to stimulate further exchange of ideas between students of these fields.

**Keywords** K<sub>2P</sub> channels • Plants • Animals

## Introduction

Two-pore domain potassium (K<sub>2P</sub>) channels are membrane proteins that have been identified in mammals and other organisms such as *Drosophila*, *Caenorhabditis elegans*, as well as different plant species [22, 30]. The functional channel is a dimer with each subunit comprising two pore-forming loops and four transmembrane domains (4TM/2P). The genome of the model plant *Arabidopsis thaliana* harbors five such genes (TPK1-5, for tandem-pore potassium, K<sup>+</sup>, named in this review, AtTPKs) that code for K<sub>2P</sub> channels. Orthologs of AtTPKs are found in all higher plants sequenced so far. In contrast, in algae, they have only been found in the chlorophyte *Ostreococcus* [71]. Although AtTPKs share their 4TM/2P topology with human K<sub>2P</sub> channels (named in this review, hK<sub>2Ps</sub>), their sequence identities and similarities are low, varying between 5.9 and 18.9 % for identity and 12.1 and 31.7 % for similarity (Online Resource 1). What did the last common ancestor (LCA) of both groups of proteins look like? Was the LCA a prokaryotic or a eukaryotic channel? What are the similarities and differences between AtTPKs and hK<sub>2Ps</sub> in

terms of their primary and tertiary structure? Are they regulated by similar or different stimuli? These questions are discussed in this review by presenting phylogenetic, structural, and experimental evidence. This approach of considering plant and animal K<sub>2P</sub> channels in the same study is novel, and both fields will certainly benefit from such mutual attention.

### Phylogenetic relationships between AtTPKs and hK<sub>2P</sub>s

Phylogenetic studies and structure/function properties of channel proteins have led to the hypothesis that the complex K<sup>+</sup> channels evolved from a simple prokaryotic precursor channel [4] or a viral-encoded K<sup>+</sup> protein [69]. Despite current arguments about the origin of all K<sup>+</sup> channels, the common precursor provided a unique pore-forming segment that resembles the pore module of modern K<sup>+</sup> channels. The tandem architecture of the K<sub>2P</sub> channels with their two-transmembrane (TM) structure (2\*2TM) probably occurred after a gene duplication of the pore module. Nonetheless, it should also be considered that the modern K<sup>+</sup> channel subunit itself may represent a functional mosaic that arose from different ancestral genes [27]. Based on the hallmark characteristic of prokaryotes to host gene clusters organized in operons, the hypothesis has emerged that a gene fusion occurred in an operon containing two K<sup>+</sup> channel genes in tandem, thus giving rise to the gene for K<sub>2P</sub> channels. In the genome of the archaea *Methanocaldococcus jannaschii*, channels exhibiting a 2TM segment and a putative NAD<sup>+</sup>-binding domain (PNBD) such as mjaKchB (MJK1) are found. MJK1 is genomically coupled in one operon to mjaKchA (MVP), a *Shaker*-like K<sup>+</sup> channel homolog with six hydrophobic segments. The 209 amino acid residues of MVP are directly followed by the first of the 333 amino acid residues of MJK1. Although there is no experimental evidence at present, a physical association between the two gene products, if stoichiometrically transcribed, is not ruled out. This would result in a tandem-pore channel [20].

In terms of organism evolution, the LCA of plants and animals is thought to have existed around 1.6 billion years (Ga) ago, the Precambrian era [66]. Information obtained from sequencing the entire genome of some plants and animals (<http://www.ncbi.nlm.nih.gov/genome/>), along with our knowledge of the function of the genes found in these genomes, points strongly towards a unicellular LCA for both kingdoms [55]. The full genome sequence of the free-living protist *Naegleria gruberi* has been used to estimate the ancestral gene families of all eukaryotes. *N. gruberi* belongs to a ubiquitous protist clade (Heterolobosea), which diverged from other eukaryotic lineages over 1 Ga ago. Analysis of the *N. gruberi* genome suggests that the LCA of existent eukaryotes had over four thousand genes that have been conserved during evolution. Forty percent of these genes may be considered

eukaryotic inventions because they have no identifiable homologs in either Archaea or Bacteria [24].

We performed BLAST searches [3] using all hK<sub>2P</sub>s and all AtTPKs as queries against the non-redundant (nr) database to find the putative LCA for both groups of proteins. The search included all available eukaryotic protein sequences, except those from the Opisthokonts, Viridiplantae, and Rhodophyta clades. Table 1 shows the BLAST search in terms of a hit in *N. gruberi*. All K<sub>2P</sub> channels match with a putative outward-rectifier potassium channel (XP\_002682402) in this organism (named NgKC in this review, from *N. gruberi* K<sup>+</sup> channel). NgKC exhibits the hallmarks of a K<sup>+</sup>-selective channel; it has two pores in tandem. The two-pore potassium channel domain (IPR013099) annotation is visibly identified by InterPro [40]. InterPro predicts the transmembrane segments of NgKC to be a similar pattern to that of the K<sub>2P</sub> channels and exhibits a clear difference from the yeast tandem-pore channel TOK1 [43], which has eight transmembrane segments (Online Resource 2). In a multiple sequence alignment (MSA) that includes NgKC, hK<sub>2P</sub>s, and AtTPKs (Online Resource 3), NgKC

**Table 1** BLAST search results of hK<sub>2P</sub>s and AtTPKs in terms of a hit in *N. gruberi*

Query	Rank	% Identity	E value
KCNK12 (THIK-2)	1	26.52	2.00E-14
KCNK13 (THIK-1)	1	24.70	5.00E-15
KCNK15 (TASK-5)	1	27.49	2.00E-11
KCNK1 (TWIK-1)	1	23.94	7.00E-10
KCNK3 (TASK-1)	1	30.91	3.00E-15
KCNK4 (TRAAK)	1	25.14	2.00E-11
KCNK9 (TASK-3)	1	31.43	1.00E-15
TOK1_YEAST	1	33.15	2.00E-16
KCNK10 (TREK-2)	2	25	1.00E-12
KCNK16 (TALK-1)	2	25	4.00E-14
KCNK17 (TALK-2)	2	24.85	6.00E-11
KCNK2 (TREK-1)	2	26.97	5.00E-13
KCNK6 (TWIK-2)	2	25.59	1.00E-11
KCNK5 (TASK-2)	3	27.54	1.00E-11
KCNK7	8	22.22	0.11
KCNK18 (TRESK)	9	25.74	0.001
TPK5	9	26.44	2.00E-09
TPK2	11	25.48	5.00E-09
TPK3	13	28.98	8.00E-08
TPK1	27	24.53	5.00E-05
TPK4	41	32.29	3.00E-05

The list is organized by the rank of NgKC as a hit in the Blastp search. The percentage of sequence identity (% identity) of the local alignments and E values produced by BLAST are also shown. In the table, the yeast channel TOK1 with six transmembrane segments, as the classical K<sub>v</sub> channels, *plus* and additional pore is also shown. For hK<sub>2P</sub>s, the systematic (HUGO) name is indicated first, followed by the conventional name

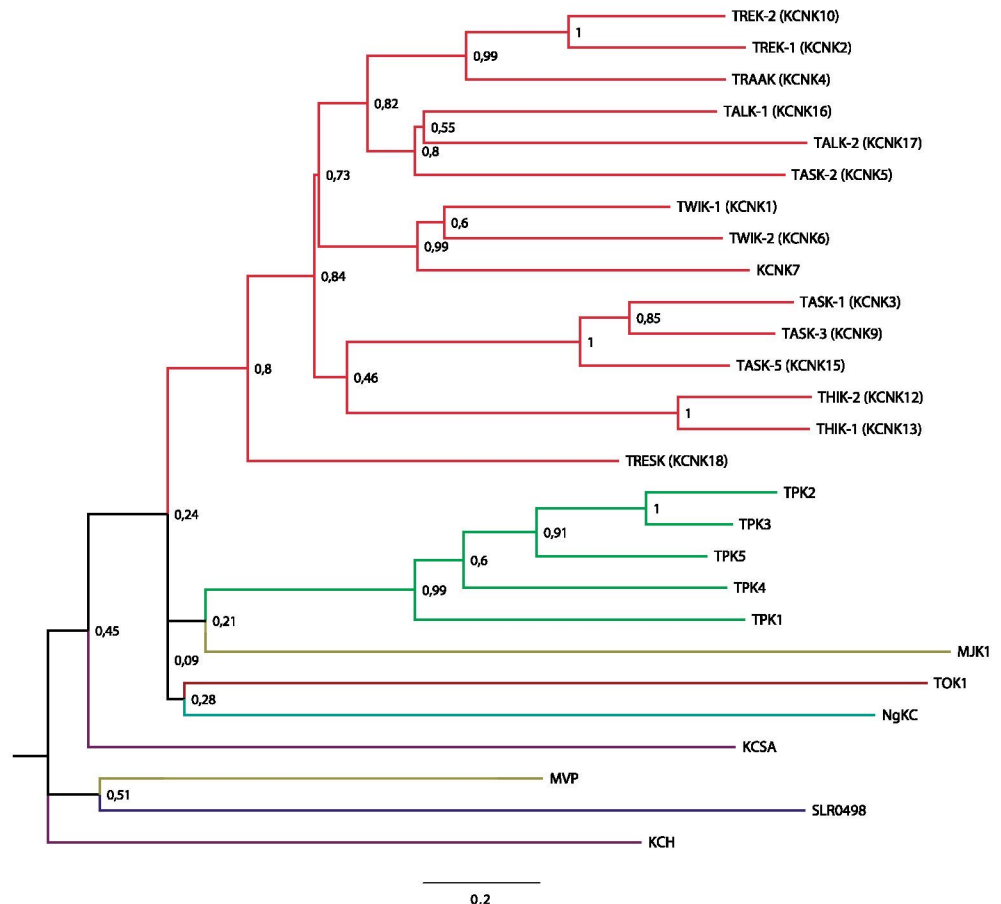
shows two pore domains (PD), each comprising an outer helix, a pore helix, a selectivity filter, and an inner helix.

Finally, a rooted phylogenetic tree was built (Fig. 1) to examine the phylogenetic relationships between  $K_{2P}$  channels in plants and animals. To test the hypothesis that a duplication event (2\*2TM) gave rise to the arrangement of  $K_{2P}$  channels in an operon with two  $K^+$  channel genes in tandem [20], we included other  $K^+$  channels in the tree, in addition to hK<sub>2P</sub>s, AtTPKs, and NgKC. Indeed, as one of the goals of the tree was to test the prokaryotic origin hypothesis suggested by Derst and Karschin [20], amino acid sequences from MVP and MJK1 channels were also included. The resulting tree resembles the evolutionary relationships among different species. Except for MJK1, which is placed in the same branch as AtTPKs, a division arose between the prokaryotic and eukaryotic  $K^+$  channels. With respect to the evolutionary relationships of eukaryotic tandem-pore  $K^+$  channels, the only anomaly is seen with the yeast channel TOK1. In the absence of lateral gene transfer, TOK1 would be expected to lie in the same branch as the opisthokont channels (hK<sub>2P</sub>s). Instead, TOK1 appears in the same branch as NgKC. The bootstrap confidence level of the nodes (i.e., the proportion of trees that confirm the nodes of the tree) reflects these inaccuracies; it decreases to the left and increases to the right of the tree. The

closer we move towards the most ancestral relationships, such as the one between prokaryotic and eukaryotic  $K^+$  channels or the divergence between the yeast channel TOK1 and NgKC, the lower the bootstrap confidence levels become (24.5 and 28.3 %, respectively). This indicates the uncertainty of these dichotomy events. In future phylogenetic analysis of  $K_{2P}$  channels, additional prokaryotic  $K^+$  channels and eukaryotic  $K_{2P}$  channel sequences should be included to explain how  $K_{2P}$  channels expanded from their ancestor precursors into the present species.

Additionally, the presence of MJK1 in the same branch of the tree as AtTPKs might be due to lateral gene transfer or could obey to the mechanism proposed by Derst and Karschin [20]. However, if a gene fusion of MVP and MJK1 channels had occurred to originate  $K_{2P}$  channels, they would have been expected to be found close to eukaryotic channels in the phylogenetic tree. Figure 1 shows that only MJK1 with one pore and a PNBD domain is close to AtTPKs, whereas MVP is in the branch of bacterial  $K^+$  channels. This suggests only MJK1 as possible precursor of  $K_{2P}$  channels and more specifically of plant TPK channels. An alternative hypothesis to that of Derst and Karschin [20] is that a gene duplication in the pore module occurred in bacteria. Nonetheless, a BLAST search did not find a channel with a tandem 2TM domain

**Fig. 1** Phylogenetic tree of representative potassium channels. In *purple*, KcsA (Uniprot ID: P0A334) and KCH (Uniprot ID: P31069) channels from Bacteria. *Yellow*, MVP (Uniprot ID: Q57603) and MJK1 (Uniprot ID: Q57604) channels from Archaea. *Blue*, SLR0498 channel from *Synechocystis* sp. PCC 6803, a Cyanobacteria (Uniprot ID: Q55815). *Cyan*, the channel NgKC (Uniprot ID: D2V059). *Brown*, the channel TOK1 (Uniprot ID: P40310). *Green*, AtTPKs; and in *red*, hK<sub>2P</sub>s. Each node is labeled with its corresponding bootstrap confidence level. The tree was obtained with ClustalW2 Phylogeny [44], using a MSA from Kalign [45]



structure in any prokaryote. Therefore, if a gene duplication event occurred, we hypothesize it took place in the eukaryotic LCA of  $K_{2P}$  channels. One of the hits found was the “outward-rectifier potassium channel” from *N. gruberi* (NgKC). This confirms that *N. gruberi* may be the evolutionary intermediate between an older eukaryotic ancestor organism and all extant eukaryotes [23].

In the tree presented here, we can see that NgKC (in cyan, Fig. 1) is close to the yeast channel TOK1. The presence of both channels in the same branch of the tree also supports the hypothesis that tandem-pore channels originated from a gene duplication in eukaryotes rather than from a gene fusion in prokaryotes. All tandem-pore channels from mammals, plants, and yeast would thus originate from a common eukaryotic ancestor. The yeast TOK1 channel could have originated subsequently by the addition of four transmembrane segments.

Perhaps the faster pace of change in prokaryotic genomes compared to eukaryotes has erased all evidence of  $K^+$  channel gene duplication events in the prokaryotic genomes. However, this idea is inadequate, given the large number of sequenced prokaryotic species. Possibly, the known and criticized bias in the classes of the prokaryote species among the sequenced genomes [73] excludes representatives that favor the hypothesis of Derst and Karschin [20]. If this were the case, the growth of sequenced genomes should reveal more information on the LCA of  $K_{2P}$  channels.

### Tertiary structure of $K_{2P}$ channels

The report from 2012 of the three-dimensional structures of TWIK-1 and TRAAK channels [14, 56] lays the foundation for further investigation of the structure of other  $K_{2P}$  channels. Through the information contained in these structures, we are in a unique position to begin to understand the three-dimensional characteristics of plant TPK channels. Three further  $hK_{2Ps}$  were subsequently reported. Brohawn et al. published a Fab-mediated crystal structure of TRAAK [13], and Pike et al. reported the structure of TREK-1 (pdb code 4TWK) and TREK-2 (pdb code 4BW5). Interestingly,  $hK_{2Ps}$  have structural features that have not been previously observed in the crystal structures of tetrameric  $K^+$  channels. It is of interest to analyze whether these features are present in AtTPKs and in NgKC.

The most salient feature (well conserved in  $hK_{2Ps}$ , Fig. 2a, b, left) is the presence of an extracellular cap (with 46 to 56 amino acids), formed by the PD1 outer helix-PD1 pore helix linker. The presence of the extracellular cap, positioned above the extracellular entrance, explains why protein toxins that block the pores of many tetrameric  $K^+$  channels from the extracellular side are ineffective against  $K_{2P}$  channels [14]. The cap also prevents direct extracellular ion access to

the selectivity filter, instead creating additional bifurcated, tunnel-like ion pathways that can accommodate hydrated  $K^+$  ions. Gonzalez et al. demonstrated that these lateral portals are involved in the extracellular pH-regulated gating of TASK-3 channel [32] and might also be important in the same process in TASK-2 [18]. The cap is not present in plant TPK channels (linker being only 5 to 20 amino acids long, Fig. 2a, b, center), which in itself is a notable difference. In view of the number of residues in the portion of sequence connecting the PD1 outer helix with the PD1 pore helix (41 amino acids, Fig. 2a, b, right), NgKC probably possesses a quasi-helical cap domain.

Another important feature found in the three-dimensional structures of TWIK-1 and TRAAK  $K_{2P}$  channels is the presence of two prominent lateral cavities or fenestrations in the intramembrane molecular surface (located between the PD1 inner helix of one subunit and PD2 inner helix of the other). The ion conduction pathway is exposed to the lipid bilayer through these openings (Fig. 2b, left). These fenestrations could be access points for endogenous lipids and hydrophobic compounds that influence ion conduction. This view is supported by the observation that the fenestrations in the TWIK-1 crystal structure are filled with electron dense material, which could be attributed to lipid alkyl chains of membrane phospholipids [56]. Analysis of the amino acids located at the fenestration could provide a clue as to whether this feature is present in AtTPKs and NgKC. The separation between the helices forming the fenestration occurs from the PD2 inner helix, being more perpendicular to the membrane plane than the PD1 inner helix. The PD1 inner helix exhibits a rigid kink at a proline residue (Pro143 in TWIK-1), being bent by approximately  $20^\circ$  at this residue. This is conserved in all  $hK_{2Ps}$ , except the THIK subfamily. The existence of a conserved proline in the PD1 inner helix thus seems to be essential for the formation of the fenestration. AtTPKs though contain a valine or glycine instead of this proline, suggesting that there is no rigid kink in the PD1 inner helix of plant channels. The proline is also absent from NgKC, which has a serine at the equivalent position. This suggests that the intramembrane fenestration might be a late acquisition in an evolution branch containing the mammalian  $K_{2P}$  channels (Fig. 2, Online Resource 3).

Recently, Aryal et al., using a protocol that combines molecular dynamics (MD) simulations with functional validation, demonstrated that TWIK-1 possesses a hydrophobic barrier deep within the inner pore and that stochastic dewetting of this hydrophobic constriction acts as a major barrier to ion conduction [7]. This could explain the low levels of functional activity of the TWIK-1 channel. The hydrophobic constriction is formed by residues present at the surface of the fenestration: Leu146 (PD1 inner helix, three residues after Pro143), Leu261 (PD2 inner helix), and Leu264 (PD2 inner helix) in TWIK-1. These create a hydrophobic cuff deep within the TWIK-1 pore. Mutations L146D, L146N, L261D,



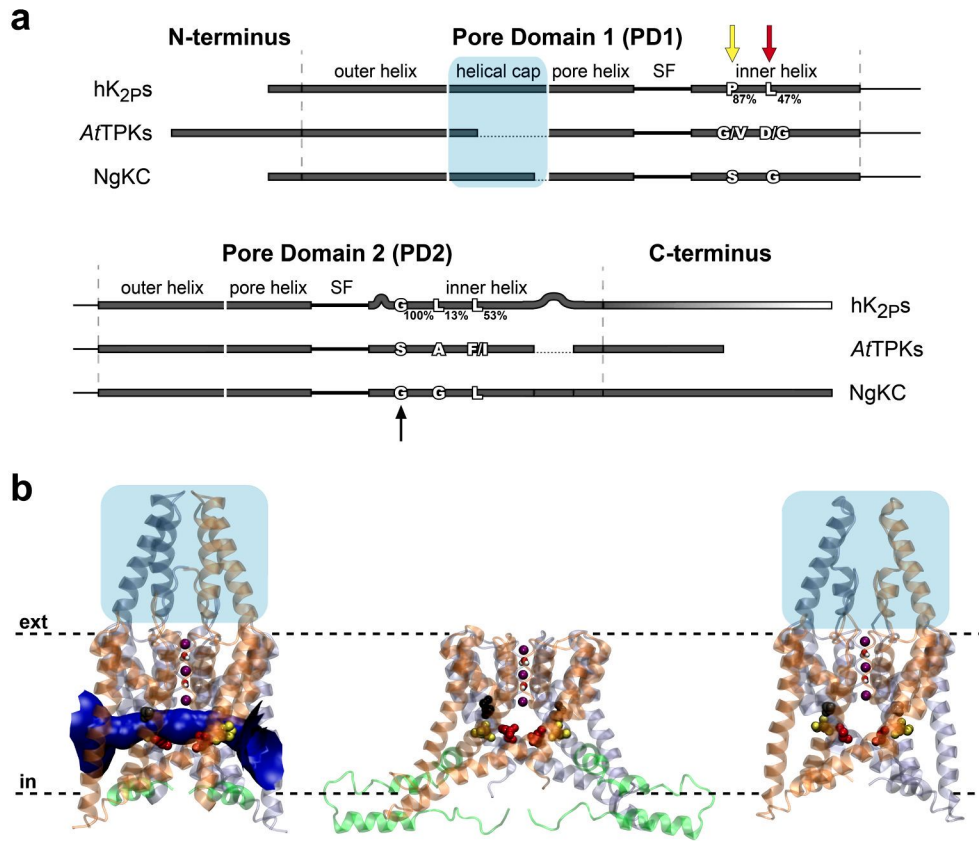


**Fig. 2** Sequence and structure comparison between hK<sub>2</sub>Ps, NgKC, and AtTPKs. **a** Simplified MSA of hK<sub>2</sub>Ps, NgKC, and AtTPKs showing the relevant features present or absent in these channels such as the helical cap (blue box), the proline position in the PD1 inner helix (yellow arrow). The Leu position—three residues after the proline of the PD1 inner helix (red arrow). The hinge glycine (black arrow) of the PD2 inner helix and, finally, the other hydrophobic positions of the PD2 inner helix found in TWIK-1 [7]. The percentage under the positions in hK<sub>2</sub>Ps represents the frequency of these amino acids between the 15 human channels. An extended MSA between hK<sub>2</sub>Ps, NgKC, and AtTPKs is shown in Online Resource 3. **b** Three-dimensional structures of the hK<sub>2</sub>P channel TWIK-1 (left, [56]), AtTPK4 (center), and NgKC (right). One subunit of the

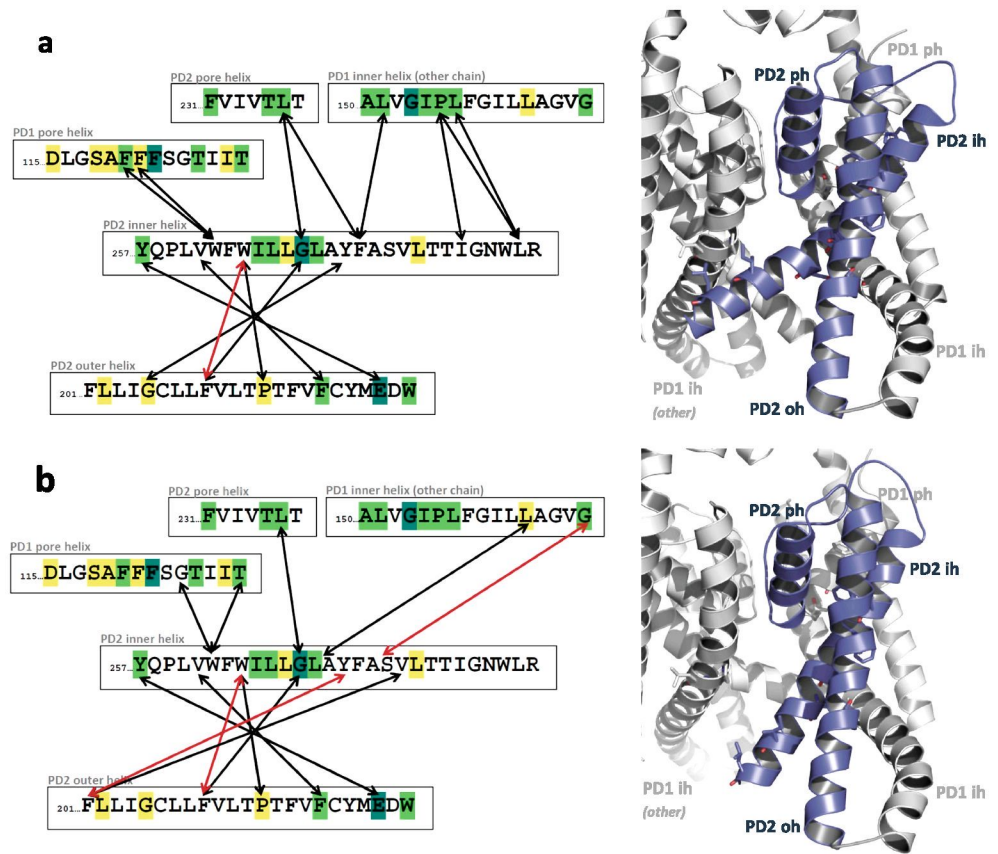
channel is represented in orange and the second in white. Potassium ions and water molecules in the selectivity filter are represented in Van der Waals. The C-helix of TWIK-1 and the C-terminus of AtTPK4 are shown in green. The AtTPK4 model was done using the ICM program [1] using as template the structure of TREK-2 (pdb code: 4BW5) for the trans-membrane section. The C-terminus was generated RaptorX server (<http://raptorx.uchicago.edu/>). The NgKC model was generated by Swiss-PDB [33] using an automatic selected template (TWIK-1). The salient features shown in **a** are here shown with the same colors. The figures were done using VMD program [39], and the fenestrations in the TWIK-1 structure were generated using HOLE [68]

and L261N in TWIK-1 resulted in large currents that were attributed to an increased hydration in the inner pore. L146 appears as the most relevant position to regulate the hydrophobicity of the conduction pathway [7]. When the alignment is analyzed, it is observed that other hydrophobic residues substitute the abovementioned leucine residues in hK<sub>2</sub>Ps, AtTPKs, and NgKC (except for TASK-2 or THIK channels, where a serine or tyrosine are respectively, Online Resource 3). But a notorious exception to this rule appears in all the AtTPKs (apart from TPK1) where position Leu146 is occupied by an aspartate. This supports the notion that there is no hydrophobic barrier deep within the inner pore of the plant K<sub>2</sub>P channels and also suggests that fenestrations are absent in these channels (Fig. 2).

Analysis of the Fab-mediated crystal structure of TRAAK showed the amino acids implicated in the opening-closing mechanism of the fenestration [13]. This structure has one of

the fenestrations completely closed. The conformational changes and differences in amino acid interactions in TRAAK when the fenestration is opened or closed are presented in Fig. 3. A comparison between the PD2 inner helix in hK<sub>2</sub>Ps, AtTPKs, and NgKC reveals more similarities than differences (Fig. 2). The hinge glycine in the PD2 inner helix of hK<sub>2</sub>Ps (Gly268 in TRAAK) is changed to a serine in AtTPKs, but is conserved as glycine in NgKC. The amino acids in the surroundings of the hinge residue (from position -4 to +5, using the hinge residue as a reference) are similar for all the K<sub>2</sub>P channels analyzed, suggesting that the movement of the PD2 inner helix of AtTPKs and NgKC is similar to that inferred for hK<sub>2</sub>Ps. Although that movement is essential to the fenestration opening in hK<sub>2</sub>Ps, it does not seem to be critical for AtTPKs and NgKC, suggested by the absence of a rigid kink (proline) in the PD1 inner helix.

**Fig. 3** Amino acid interactions in both subunits of the Fab-mediated crystal structure of TRAAK. **a** Subunit that contains the closed fenestration. **b** Subunit with the opened fenestration. Fully conserved amino acids in hK<sub>2P</sub>s are highlighted in *blue*, highly conserved amino acids in *green*, and partially conserved amino acids in *yellow*. Red arrows represent hydrogen bonds, and black arrows represent non-bonding interactions between the amino acids. PD1 and PD2 mean pore domain 1 and 2, respectively. *ih* and *oh* mean inner helix and outer helix, respectively. PD1 *ih* (*other*) means the pore domain inner helix 1 from the other subunit



A further potentially important feature is found in the three-dimensional structure of TWIK-1. An amphipathic “C-helix” with a proposed role in gating is located at the distal end of the PD2 inner helix and runs parallel to the cytosolic face of the membrane (Fig. 2a) [56]. The so-called C-helix goes from His271 to Tyr 281 of TWIK-1 and is absent from the crystal structures of TRAAK and TREK channels. Given the number of residues at the distal end of the PD2 inner helix prior to the C-terminus (see dashed lines after the PD2 inner helix in Online Resource 3), it is probable that only the TWIK subfamily of human K<sub>2P</sub> channels possess the C-helix. AtTPKs do not show amino acids within the C-helix region, and NgKC shows only five residues.

### Experimental evidence of similarities and differences between plant and animal K<sub>2P</sub> channels

Animal K<sub>2P</sub> channels are well known as potassium background or “leak” channels that exhibit voltage-independent gating and are constitutively open at rest. Nevertheless, these channels are subject to regulation by diverse chemical and physical factors such as extracellular and cytosolic pH, polyunsaturated fatty acids (PUFAs), phosphorylation, volatile anesthetics, mechanical forces, and temperature [22, 37, 61]. Animal K<sub>2P</sub> channels

are grouped into six different classes according to their sequence similarity and stimulus susceptibility. As shown above (Fig. 1), TWIK-1 (KCNK1), TWIK-2 (KCNK6), and KCNK7 channels that operate as weak inward rectifiers comprise the first subfamily. Subfamily 2 encompasses the mechano-gated channels TREK-1 (KCNK2), TREK-2 (KCNK10), and TRAAK (KCNK4), while TASK-1 (KCNK3), TASK-3 (KCNK9), and TASK-5 (KCNK15) channels denote the acid-inhibited channels of subfamily 3. The THIK-1 (KCNK13) and THIK-2 (KCNK12) channels constitute branch 4 and are inhibited by the volatile anesthetic halothane. Subclade 5 contains K<sub>2P</sub> channels activated by alkaline pH and includes TALK-1 (KCNK16), TALK-2 (KCNK17), and TASK-2 (KCNK5). The TWIK-related spinal cord K<sup>+</sup> (TRESK, KCNK18) channel, which is regulated by intracellular calcium, represents the only member of subgroup 6. While the properties of animal K<sub>2P</sub> channels in terms of biophysics as well as structure and function have been characterized to some extent, much less is known about their orthologs in plants (TPKs). This lack of knowledge is probably attributed to the intracellular localization of most of the plant K<sub>2P</sub> channels, so challenging experimental accessibility. Among the five TPK channels (TPK1-5) from the model plant *A. thaliana*, only AtTPK4 appears localized to the plasma membrane; all other members are reported as targeted to the plant lytic compartment—the vacuole [6, 41, 71].



## Targeting of K<sub>2P</sub> channels

Animal K<sub>2P</sub> channels exerting their function at the plasma membrane of neuronal cells control the resting membrane potential and electrical excitability. Post-translational regulation of K<sub>2P</sub> protein trafficking feeds back on the channel number and density, thus determining the functional properties of these neurons. Many K<sub>2P</sub>-interacting proteins have been identified, and some of them are related to channel trafficking [54]. Binding of 14-3-3 proteins to the extreme C-terminal region of TASK1 and TASK3 has been reported to promote their surface expression. This binding site, a dibasic motif (RR(K/S)S<sub>p</sub>V), is reminiscent of a similar 14-3-3 binding motif (RR(S/C)RS<sub>p</sub>A) found in plant TPK1-like channels [46]. Although 14-3-3 binding to Arabidopsis TPK1 has different functions to those seen with TASK channels (see below), in both cases, phosphorylation of the distal serine was shown to be essential for 14-3-3 binding [46, 60]. In contrast to 14-3-3 proteins, which promote TASK plasma membrane expression, the interaction between coatamer protein complex 1 (COPI) and TASK channels leads to decreased surface expression and accumulation of channels in the endoplasmic reticulum (ER) [74]. Thus, the antagonistic action of COPI and 14-3-3 provide a means to either retain TASK channels in the ER (for COPI) or promote TASK channel trafficking towards the membrane (with 14-3-3 proteins).

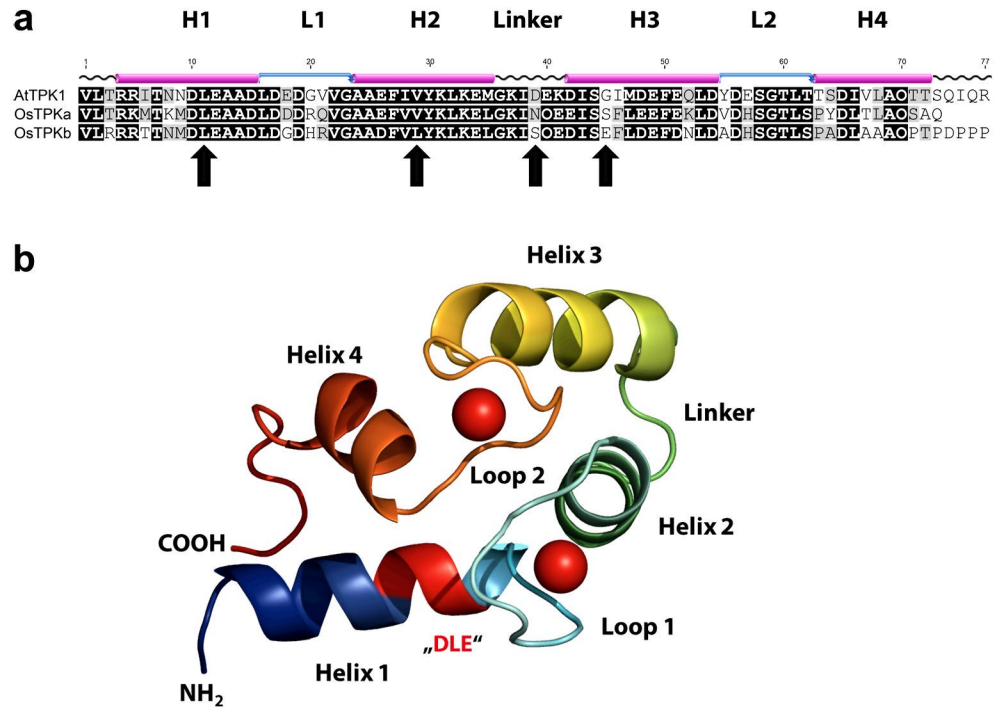
Although plant cells are excitable and use ion channels to generate electrical signals to communicate and sense environmental changes, they lack neurons in the proper sense. Plants though possess a bi-directionally operating vascular tissue named phloem, which is proposed to fulfill a role in long-distance transport of solutes as well as in electrical signaling (see below). Furthermore, potassium is a major plant nutrient and the majority of cellular K<sup>+</sup> resides in the vacuole. Plant growth, development, and movements are based on osmotic phenomena, with potassium ions being one of the most important osmolytes building up cell turgor. Thus, plant K<sub>2P</sub> channels of the TPK clade expressed in the vacuolar membrane (tonoplast) play an important role in maintaining cellular K<sup>+</sup> homeostasis. Based on structure-function studies and domain swapping experiments between the Arabidopsis PM-localized AtTPK4 channel and the vacuolar AtTPK1, the C-terminus of the latter was identified as the major determinant for vacuolar targeting [21, 51]. AtTPK1 contains two EF hands in its C-terminus, which exhibit structural homology to the neuronal Ca<sup>2+</sup>-binding protein calcineurin (Fig. 4). A TPK1 mutant lacking the entire C-terminal domain (TPK1-ΔCT) was retained in the ER, while those possessing helix H1 in the EF-hand 1 (TPK1-ΔL1) escaped from the ER and partially entered the Golgi stacks. Extending the AtTPK1 CT to include the H1-L1 region (TPK1-ΔH2) accelerated ER export and proper targeting to the vacuolar membrane. A more detailed analysis of the H1-L1 region identified a di-acidic motif (“DLE”) as vital for efficient ER export of the Arabidopsis TPK1 channel. Likewise, a di-acidic motif (EDE) in the proximal C-

terminus of TASK-3 was shown to play a crucial role in trafficking these channels to the plasma membrane through interactions with the COPII complex [75]. In TASK3, this di-acidic ER retention motif is masked upon 14-3-3 binding to the late C-terminus of the channel, thus promoting TASK3 surface expression. In contrast, in TPK1, the 14-3-3 binding site is located at the N-terminus and was shown to be involved in the regulation of channel activity rather than in channel trafficking [21, 42]. Like AtTPK1, its Arabidopsis homologs AtTPK2, 3, and 5 also localize to the lytic vacuole (LV) and, to a lesser extent, are also expressed in smaller, vesicle-like structures, which could represent protein storage vacuoles (PSV). Indeed, the rice genome (*Oryza sativa*) encodes two TPK orthologs, designated OsTPKa and b, which exhibit substantial homology to AtTPK1. Studies by the group of Frans Maathius have shown that OsTPKa is expressed in the LV compartment while OsTPKb localizes to the PSV [42]. Three critical residues, L303, S313, and N326 (see Fig. 4), located between the core motifs of the two EF hands in the cytoplasmic C-terminus of the rice TPK channels, were identified in a survey addressing the molecular mechanisms of differential channel targeting. The Arabidopsis TPK3 appears exceptional among the plant TPK channels since it exhibits dual targeting. Besides its expression in vacuoles, a recent report provides evidence for localization in the photosynthetic membrane (thylakoid) of chloroplasts [16]. AtTPK3 seems to regulate photosynthesis efficiency (see below), but the molecular mechanisms underlying the dual targeting phenomenon remain elusive and need to be addressed.

## TPK channels are K<sup>+</sup> selective “weak rectifiers”

Cloning of the first plant potassium channels became feasible at the beginning of the 1990s by complementing K<sup>+</sup> transport-deficient yeast strains [5, 67]. Although this approach was initially employed for the characterization of Shaker-like, voltage-dependent K<sup>+</sup> uptake channels [11], the Arabidopsis plasma membrane localized TPK4 channel was the first K<sub>2P</sub> channel proven to complement yeast growth under potassium-limiting conditions [9, 10]. AtTPK4 mediated growth rescue at 100 μM potassium, while the vacuolar localized AtTPK1 failed to restore yeast growth at low external K<sup>+</sup> concentrations. Patch-clamp analysis of TPK4 expressed in yeast plasma membrane allowed the characterization of this channel as a K<sup>+</sup> selective “weak inward rectifier” with a slope conductance of 77 pS (195/150 mM KCl), as determined from single-channel recordings. These findings perfectly matched the basic biophysical properties of AtTPK4 when functionally expressed in *Xenopus laevis* oocytes. AtTPK1 was shown to exhibit similar properties to AtTPK4 when functionally expressed in a yeast mutant lacking the endogenous vacuolar channel YFC1 [12]. Channel currents of AtTPK1-expressing yeast vacuolar membranes displayed weak asymmetry, showing larger inward currents—favoring

**Fig. 4** Structural motifs in the C-terminal EF hands of plant  $K_{2P}$  channels involved in channel targeting and regulation. **a** Alignment of the EF hand containing carboxy-termini of AtTPK1 and its rice orthologs. Arrows denote residues identified as being involved in vacuolar targeting. **b** Structure of the  $Ca^{2+}$ -binding EF hands of the Arabidopsis vacuolar TPK1 channel highlighting the “DLE” ER retention motif



cation fluxes from the vacuole into the cytosol—and smaller outward currents that saturate at depolarizing voltages. Single-channel conductance in symmetrical 100 mM  $K^+$  was 75 pS for the inward currents and 40 pS for the outward currents. Only inward currents were detected under bi-ionic conditions with 100 mM KCl on the vacuolar side and 100 mM NaCl on the cytosolic side, demonstrating a strong selectivity for  $K^+$  over  $Na^+$  of TPK1. These results were finally confirmed by in vivo electrophysiological studies on Arabidopsis vacuoles, thus fully elucidating the TPK1 function [49]. The main conductance in plant vacuoles is attributed to the action of the “slow activating vacuolar” (SV) channel, encoded by the *TPC1* gene [36, 72]. Hence, a double-mutant lacking AtTPC1 and AtTPK1 (*tpc1 x tpk1*) was employed to re-introduce and characterize the AtTPK1 channel [28]. Based on patch-clamp studies on isolated Arabidopsis vacuoles, AtTPK1 was characterized as a strongly  $K^+$  selective, weak rectifier, exhibiting an inward unitary conductance of 45 pS and an outward conductance of 20 pS. These studies therefore identified AtTPK1 as the “vacuolar  $K^+$ ” (VK) channel. Although the functional expression of TPK2, TPK3, and TPK5 in the Arabidopsis *tpc1 x tpk1* mutant has so far not been successful [42], a domain-swapping approach between the PM-localized AtTPK4 and these channels provided evidence for their function as  $K^+$  selective ion channels. When replacing the second pore of AtTPK4 with the homologous region of either of the vacuolar TPK channel (except for TPK1), instantaneous,  $K^+$  selective, “weakly rectifying” currents were recorded in *Xenopus* oocytes [52].

The yeast heterologous expression system was also shown to be a valuable tool for the electrophysiological characterization of

the AtTPK1 ortholog in tobacco (*Nicotiana tabacum*) [34]. Like its congener from Arabidopsis, NtTPK1b was highly selective for  $K^+$  over  $Na^+$ , but apparently lacked the rectification properties previously observed in AtTPK1. As well as NtTPK1b, tobacco also expresses an additional TPK isoform, designated NtTPK1a. Remarkably, and different from many other TPK channels, NtTPK1a possesses a “GHG” rather than a “GY/FG” motif in the second pore region. Expression of NtTPK1a as well as NtTPK1b nevertheless rescued growth of a  $K^+$  transport impaired *Escherichia coli* strain (LB2003) [34]. Surprisingly, mutating the second pore region of NtTPK1a from “GHG” to “AAA” still allowed for  $K^+$ -dependent growth, while the first pore region point mutants failed to complement the  $K^+$  uptake deficiency. The authors concluded that the second pore region in NtTPK1a is not essential for transport. The fact that AtTPK3 and AtTPK5 are capable of complementing  $K^+$  uptake deficiency in *E. coli* LB2003 also suggests that all plant  $K_{2P}$  channels represent instantaneously activating, voltage-independent  $K^+$  selective channels.

## Post-translational regulation of TPK channels

### Protons

Animal  $K_{2P}$  channel gating is subject to regulation by extracellular and intracellular pH [22, 37]. In comparison, relatively little is known about the regulation of plant  $K_{2P}$  channels (TPKs) by pH. The only PM-localized plant TPK channel, AtTPK4, has been studied by means of patch-clamp, as well as two-electrode-

voltage-clamp (TEVC) techniques following heterologous expression in *Xenopus* oocytes. It was found that this instantaneous weak inward rectifier was extraordinarily sensitive to cytoplasmic acidification [10]. Intracellular acidification by bath perfusion of AtTPK4-expressing oocytes with 10 mM sodium acetate resulted in complete inhibition of the channel currents within 100 s. Furthermore, patch-clamp analysis revealed that acidification drastically reduces the open probability of AtTPK4 and further demonstrated that intracellular proton-mediated inhibition is fully reversible. This feature of AtTPK4 is reminiscent of acidification-inhibition of the animal  $K_{2P}$  channels TWIK-1 and TWIK-2 [22, 48] in contrast to TREK-1 and TREK-2 that are activated by acidification [38]. The pronounced  $pH_i$  sensitivity of TPK4 became apparent when concomitant to the electrophysiological recording a pH-sensitive microelectrode was used to follow the kinetics of acetate-mediated changes of intracellular  $[H^+]$  in the oocyte. These studies showed that a change of the oocyte resting pH of about 0.3 pH units (7.5 to 7.2) was sufficient to fully inhibit TPK4 currents. Although histidine residues have often been implicated in the proton sensitivity of potassium channels [6, 35], mutational analyses of the corresponding cytosolic-localized residues excluded this possibility for AtTPK4 (own unpublished results).

Similarly, the vacuolar-localized AtTPK4-homolog, AtTPK1, is sensitive to changes in  $[H^+]_i$ . AtTPK1 open probability exhibits a maximum at a cytosolic pH of around 6.7, reducing steeply towards more alkaline pH values [28]. Since the channel activity also moderately decreased at a more acidic pH, the authors concluded that at a physiological pH (~7.5–7.8), the TPK1 open probability would only reflect 20–30 % of the maximum open probability. These results further suggest an additional, superior regulatory mechanism for AtTPK1 (see below). In contrast to the Arabidopsis TPK1, the pH profile of its ortholog from tobacco, NtTPK1 seems different [34]. NtTPK1, when expressed in yeast vacuoles, was activated at an acidic cytosolic pH, exhibiting an  $EC_{50}$  of about pH 6.0. In both cases, however, the molecular mechanism of cytosolic pH sensing is unknown.

The activity of members of the TREK subfamily is also modified by intracellular pH changes [22]. Protons activate both TREK-1 and TREK-2, but not TRAAK. In TREK-1 and TREK-2 channels, the intracellular proton sensor appears to be composed of a 30-amino-acid stretch in the proximal C-terminal intracellular domain, which contains a critical glutamate residue [38]. Whether a similar mechanism controls the acid-inhibited Arabidopsis TPK4 remains to be elucidated. In contrast to regulation by intracellular pH, AtTPK4 is insensitive to changes in the external (apoplastic) proton concentration, a feature that distinguishes the plant  $K_{2P}$  channel from the plant Shaker-like  $K^+$  uptake channels, as well as from its animal orthologs TREK-1, TREK-2, or members of the TASK and TALK subfamily. Plant Shaker channels of the KAT1 subfamily are activated by extracellular acidification; increasing  $[H^+]_{ext}$  increases the open probability ( $P_o$ ) of these hyperpolarization-activated, voltage-

dependent channels by shifting the activation curve positively along the voltage axis [6, 35]. Histidine residues located in the extracellular transmembrane linker regions, as well as in the selectivity filter, were shown to constitute the external pH sensor in these channels or, alternatively, a sensory cloud rather than single key amino acids [31]. Likewise, extracellular-located histidine residues were identified as extracellular proton sensors in the TASK-1, TASK-3, and TREK-1 channel; all were inhibited by extracellular acidification [19, 32]. The pH sensitivity of TASK and TREK-1 channels is steep, and proton-mediated channel shutdown occurs after a change within one pH unit, starting from physiological extracellular pH levels (e.g., 7.4 to 6.4) [65]. Despite its high homology to TREK-1, in TREK-2, a corresponding histidine located in the M1P1 extracellular loop that precedes the first P domain confers activation rather than inhibition of this channel by extracellular acidification. Based on site-directed mutagenesis studies, it was concluded that the opposite actions of histidine protonation in both channels are due to different types of electrostatic interactions between this histidine and non-conserved residues in the P2-M4 interdomain of TREK-1 and TREK-2. In channels of the TALK family (TASK-2, TALK-1, and TALK-2), which are activated by extracellular alkalinization in the pH 7.5–10 range, the pH sensitivity depends on a single positively charged amino acid (R/K) located in the vicinity of the second pore domain [58, 59].

## Calcium

Calcium represents a common second messenger in both animals and plants. Calcium is central to many signal transduction networks involved in adaptive responses and developmental programs, and calcium-dependent regulation of animal  $K_{2P}$  channels has been reported. The effects appear, however, indirect and seem to rely mainly on G-protein receptor signaling [22]. This observation is in line with a lack of  $Ca^{2+}$  binding motifs (e.g., EF hands) in the sequence of the animal  $K_{2P}$  channels. Except for AtTPK4, all other members of the plant  $K_{2P}$  family, the vacuolar-located TPK channels, appear to exhibit canonical  $Ca^{2+}$  binding EF hands in the carboxy terminal domains [71]. Direct  $Ca^{2+}$  binding was shown for the cytosolic localized EF hands of the AtTPK1 channel [46]. In line with this observation, changes in luminal calcium concentrations did not impinge upon channel activity, but cytosolic calcium increased or removal of calcium prevented AtTPK1 currents [12, 46]. Patch-clamp studies on plant vacuoles (*tpk1 x tpc1*, see above) overexpressing AtTPK1 revealed an apparent effective concentration ( $EC_{50}$ ) of about 10  $\mu M$   $Ca^{2+}$  for AtTPK1 activation [28]. In view of the low open probability at physiological cytosolic pH values (~7.5–7.8, see above), elevations in the cytosolic calcium concentration seem to represent the key mechanism for Arabidopsis TPK1 activation in response to change environmental conditions. Although the tobacco TPK1 channel exhibits a predicted EF-hand motif in its C-terminal region, increasing



$\text{Ca}^{2+}$  from nominally zero to 45  $\mu\text{M}$  in the bath solution led to an only twofold activation of NtTPK1 currents. Thus,  $\text{Ca}^{2+}$  sensitivity of NtTPK1 is rather low compared to that of AtTPK1 [34].

#### Mechanical forces and temperature

TREK and TRAAK channels constitute the paradigm of  $\text{K}_{2\text{P}}$  channels activated by mechanical forces [15, 22, 37]. Negative pressure applied through a patch pipette in the cell-attached configuration was shown to reversibly activate TREK-1, TREK-2, and TRAAK. In TREK-1, a sigmoidal relationship between the channel activity and pressure defines a half-maximal activation at about  $-50$  mmHg. Since the number of active TREK-1 channels increased even in the presence of cytoskeleton-destabilizing agents, it was hypothesized that mechanical forces are likely to be transmitted through the membrane bilayer itself [37]. This hypothesis has recently been corroborated in a study showing that positive as well as negative pressure activates recombinant TRAAK and TREK-1 channels reconstituted in proteoliposomes [15]. Thus, mechano-gated  $\text{K}_{2\text{P}}$  channels probably act as sensors of membrane tension, so cell volume. Likewise, the activity of TPKs from Arabidopsis, rice, and barley (33) was shown to be regulated by membrane stretch and osmotic gradients [49]. Although not as sensitive as its animal orthologs, the activity of AtTPK1 increased by about twofold upon applying negative pressure (suction) to the membrane. All plant TPK channels tested in this study appeared mechanosensitive, with the barley HvTPK1 channel exhibiting the highest sensitivity. In line with their mechanosensitivity, plant TPK channels respond to transvacuolar osmotic changes. Channel activity is most notably increased under hypoosmotic stress conditions when the luminal osmolarity is increased with respect to the cytoplasmic compartment. The idea that activation of osmosensitive TPKs provides for the rapid release of  $\text{K}^+$  from the vacuole is supported by the finding that *tpk1* loss-of-function mutants exhibit higher sensitivity towards osmotic shock compared to wild-type cells. In addition, mechanosensitivity extends to transcriptional regulation; tobacco TPK channel transcripts are upregulated in response to salt stress or high osmotic shock [34, 46]. In contrast to vacuolar TPK channels, the PM-localized TPK4 channel is only moderately sensitive to membrane stretch. AtTPK4-mediated inward currents in *Xenopus* oocytes were reversibly increased by up to only 30 % under hypoosmotic conditions [10]. AtTPK4, as TREK-1, was shown to be temperature-sensitive exhibiting a  $Q_{10}$  of 3.6 for temperatures  $>20^\circ\text{C}$  and a  $Q_{10}$  of 1.7 for temperatures  $<20^\circ\text{C}$  [10, 50]. Thus, it is about half as sensitive as TREK-1 [50]. For TREK channels, it was shown that the C-terminal domain together with transmembrane helix M4 and pore helix 1 are crucial for temperature sensing [8, 22, 50]. Whether this holds true for the plant TPK channels or whether temperature-dependent gating is mediated by multiple temperature-sensing microdomains distributed over the whole channel protein [17] remains to be elucidated.

#### Phosphorylation and accessory proteins

Many reports have demonstrated the regulation of animal  $\text{K}_{2\text{P}}$  channels through phosphorylation. TREK-1 and TREK-2 activities, for example, are inhibited upon channel phosphorylation by the kinases PKA or PKC, and it seems that this plays a pivotal role during G-protein-coupled receptor stimulation (Gs or Gq) [22]. Conversely, TREK activity is enhanced through dephosphorylation by the protein phosphatase calcineurin, counteracting the PKA/PKC-mediated inhibition [53]. In contrast, control of plant  $\text{K}_{2\text{P}}$  channels through reversible phosphorylation/dephosphorylation is largely unexplored. Many vacuolar TPK channels exhibit a conserved 14-3-3 motif in their N-terminal domain [6, 71]. Binding of 14-3-3 proteins to, for example, AtTPK1 increases channel activity, so represents an additional, superior regulatory mechanism for vacuolar TPK channels [41, 46]. This effect of 14-3-3 proteins is in contrast to what is observed for animal  $\text{K}_{2\text{P}}$  channels. Here, 14-3-3s seem to be involved in the regulation of channel surface expression rather than its activity. Interaction of 14-3-3 proteins with plant TPKs requires the phosphorylation of conserved Ser/Thr residues within the 14-3-3 binding motif. Our studies provide evidence that phosphorylation of TPK1 involves  $\text{Ca}^{2+}$ -dependent kinases from the CPK family [47].

#### Functional implications of the comparison of animal and plant $\text{K}_{2\text{P}}$ s channels

Despite their structural homology, animal and plant  $\text{K}_{2\text{P}}$  channels exert different physiological functions. Active animal  $\text{K}_{2\text{P}}$  channels give rise to leak (background)  $\text{K}^+$  currents. By “clamping” a negative resting membrane potential close to the equilibrium potential ( $E_{\text{K}}$ ) for potassium, so below the threshold for firing action potentials, these channels in most cases suppress electrical excitability [22, 29]. Although plants are well known for firing action potentials in response to various external stress stimuli [25] and probably employ them for communicating “danger” signals across long distances [57] [62], there clearly is no evidence for structures such as neurons or synapses in plants [2]. Action potentials are accompanied by  $\text{K}^+$  fluxes across the plasma membrane. TPK4 is the only plasma membrane-localized TPK channel and is expressed just in pollen [10]. Plasma membrane-localized Shaker-like  $\text{K}^+$  efflux channels thus likely contribute to the repolarization phase of plant action potentials, and it is well feasible that TPK-mediated vacuolar  $\text{K}^+$  efflux contributes to it, although this has not been shown so far. Since in most plants action potentials are restricted to phloem tissue, the general role of ubiquitous expressed plant  $\text{K}_{2\text{P}}$  channels of the TPK family however is likely to be related to potassium



homeostasis. This is especially evident for the vacuolar potassium channels. The vacuole represents an important storage organelle for potassium, and TPK-mediated  $K^+$  release into the cytosol represents an important mechanism in balancing cytosolic potassium concentrations to provide for growth and movements, as well as during conditions of, for example, salt stress or  $K^+$  limitation [5 and references therein]. The instantaneously activating TPK channels could also be considered as part of a “ $K^+$  battery,” assisting proton-coupled transport processes. This idea was originally proposed for the weakly rectifying Shaker-like channels (AKT2, ZMK2) expressed in the phloem, the bidirectional operating long-distance transport tissue of plants [26, 62]. These studies showed that  $K^+$  circulating in the phloem serves as a decentralized energy storage that can be used to overcome local energy limitations. Plants employ ATP-driven proton pumps to build up a  $H^+$  gradient, which then serves as a secondary energy source driving the uptake of sugars and amino acids through  $H^+$ -coupled symporters. Active  $H^+$ -coupled sugar transport into the phloem cells results in depolarization of the membrane potential, which decreases the driving force for sugar uptake. In their non-rectifying mode, AKT2/ZMK2 channels enable a passage for  $K^+$  efflux concomitant to  $H^+$  uptake, thereby clamping the resting potential negative (close to  $E_K$ ) and assisting the plasma membrane proton pump in energizing transmembrane loading processes. A similar situation is found in fast polar growing pollen tubes where AtTPK4 is expressed [10]. Pollen tube growth is driven by an osmotic machinery comprising the proton pump, sugar transporters, and  $K^+$  channels, including AtTPK4. The voltage-independent, instantaneously active AtTPK4 uses the  $K^+$  gradient to complement the  $H^+$  gradient built up by the  $H^+$ -ATPase. Transporter-mediated uptake of protons (in symport with sugars) leads to cytosolic acidification in the vicinity of the proton-sensitive AtTPK4 channel. This decreases channel activity, providing a means to fine-tune the driving force for sugar uptake, thus preventing rupture of the fragile pollen tube tip. Photosynthesis in plants also depends on a proton gradient (proton motif force, PMF), which in chloroplasts is used to convert light energy into the production of ATP. The Arabidopsis TPK3 channel located in the thylakoid membrane of chloroplasts sustains the PMF by counterbalancing the light-dependent acidification of the thylakoid lumen through  $K^+$  efflux, thus optimizing ATP synthesis [16]. Whether, in addition to their role in  $K^+$  homeostasis, vacuolar TPK channels exert similar functions in aiding vacuolar secondary transport processes is not known. Likewise, the putative role of animal  $K_{2P}$  channels as part of a  $K^+$  battery, so regulators of sodium-coupled transporters, has not been addressed so far.

A role for lipids in regulating plant  $K_{2P}$  channels has not yet been demonstrated and probably can be neglected (own unpublished results). Although arachidonic acid is not commonly found in plants, they do share analogous fatty acid (FA)

signaling systems with animals. In particular, FA oxidation products called oxylipins (plants) and eicosanoids (animals) are employed in stress signaling cascades. Plant oxylipins are derived from oxidation products of linolenic acid (LA) with the phytohormone jasmonic acid (JA) representing the major product of this pathway. JA regulates a number of developmental processes, as well as stress responses, and the biosynthesis of oxylipins is triggered by, for instance, herbivore attack, wounding, and, interestingly,  $K^+$  deficiency [70]. Oxylipin biosynthesis is linked to the activity of the slow vacuolar, two-pore channel TPC1. The *fou2* mutant, which represents a point mutation in TPC1, is characterized by increased JA levels [36]. Currently, the functional link between TPC1, wounding, or potassium starvation and oxylipin biosynthesis is scant. It is tempting to speculate though that other potassium permeable channels, including the vacuolar TPK channels, comprise part of this signaling network.

Finally, in comparison to animal  $K_{2P}$  channels, little is known about the gating processes of TPK channels in plants. Structure-function analyses aided by molecular modeling would thus provide novel insights into the activation/deactivation mechanisms of these channels [63]. Based on the available structures [7, 13, 14, 56], molecular modeling-assisted domain swapping and generation of chimera between animal and plant channels could help to elucidate the enigmatic role of, for example, C-terminal domains in  $K_{2P}$  channel regulation by lipids, calcium, and/or pH. Taken together, it can be expected that comparative studies on animal and plant  $K_{2P}$  channels will move the field forward and broaden our knowledge on the evolution, physiological role, and molecular mechanisms of the regulation of these fascinating classes of ion channels in all branches of the tree of life.

**Acknowledgments** This work was supported by the Comisión Nacional Científica y Tecnológica from Chile (grants DAAD-Conicyt-2012 to WG, JC, MJ, and DB; Fondecyt #1140624 to WG and BV; ACT1104 to WG and JR; Fondef Idea CA13I10223 to WG and LZ; and Fondecyt #11110217 to LZ. The Centro de Estudios Científicos (CECs) is funded by the Centres of Excellence Base Financing Programme of CONICYT). Funding of DB and MJ by the DFG Research Training Group (Graduiertenkolleg) GRK 1342 is greatly acknowledged. We thank Tracey Ann Cuin for the critical reading of and helpful comments on the manuscript and Javier Sánchez-Contreras for managing the bibliography.

**Conflict of interest** The authors declare no conflict of interest.

## References

1. Abagyan R, Totrov M, Kuznetsov D (1994) ICM—a new method for protein modeling and design: applications to docking and structure prediction from the distorted native conformation. *J Comput Chem* 15:488–506. doi:10.1002/jcc.540150503
2. Alpi A, Amrhein N, Bertl A, Blatt MR, Blumwald E, Cervone F, Dainty J, De Michelis MI, Epstein E, Galston AW, Goldsmith MH,

- Hawes C, Hell R, Hetherington A, Hofte H, Juergens G, Leaver CJ, Moroni A, Murphy A, Oparka K, Perata P, Quader H, Rausch T, Ritzenthaler C, Rivetta A, Robinson DG, Sanders D, Scheres B, Schumacher K, Sentenac H, Slayman CL, Soave C, Somerville C, Taiz L, Thiel G, Wagner R (2007) Plant neurobiology: no brain, no gain? *Trends Plant Sci* 12:135–136. doi:10.1016/j.tplants.2007.03.002
3. Altschul SF, Gish W, Miller W, Myers EW, Lipman DJ (1990) Basic local alignment search tool department of computer science. *J Mol Biol* 215:403–410. doi:10.1016/S0022-2836(05)80360-2
4. Anderson PA, Greenberg RM (2001) Phylogeny of ion channels: clues to structure and function. *Comp Biochem Physiol B Biochem Mol Biol* 129:17–28. doi:10.1016/S1096-4959(01)00376-1
5. Anderson JA, Huprikar SS, Kochian LV, Lucas WJ, Gaber RF (1992) Functional expression of a probable *Arabidopsis thaliana* potassium channel in *Saccharomyces cerevisiae*. *Proc Natl Acad Sci U S A* 89:3736–3740. doi:10.1073/pnas.89.9.3736
6. Anschütz U, Becker D, Shabala S (2014) Going beyond nutrition: regulation of potassium homeostasis as a common denominator of plant adaptive responses to environment. *J Plant Physiol* 171:670–687. doi:10.1016/j.jplph.2014.01.009
7. Aryal P, Abd-Wahab F, Bucci G, Sansom MSP, Tucker SJ (2014) A hydrophobic barrier deep within the inner pore of the TWIK-1 K2P potassium channel. *Nat Commun* 5:1–9. doi:10.1038/Ncomms5377
8. Bagriantsev SN, Clark KA, Minor DL (2012) Metabolic and thermal stimuli control K(2P)2.1 (TREK-1) through modular sensory and gating domains. *EMBO J* 31:3297–3308. doi:10.1038/Emboj.2012.171
9. Bagriantsev SN, Minor DLJ (2013) Using yeast to study potassium channel function and interactions with small molecules. *Methods Mol Biol* 995:1–10. doi:10.1007/978-1-62703-345-9\_3
10. Becker D, Geiger D, Dunkel M, Roller A, Bertl A, Latz A, Carpaneto A, Dietrich P, Roelfsema MRG, Voelker C, Schmidt D, Czempinski K, Hedrich R (2004) AtTPK4, an *Arabidopsis* tandem-pore K<sup>+</sup> channel, poised to control the pollen membrane voltage in a pH- and Ca<sup>2+</sup>-dependent manner. *PNAS* 101:15621–15626. doi:10.1073/pnas.0401502101
11. Bertl A, Reid JD, Sentenac H, Slayman CL (1997) Functional comparison of plant inward-rectifier channels expressed in yeast. *J Exp Bot* 48:405–413. doi:10.1093/jxb/48.Special\_Issue.405
12. Bihler H, Eing C, Hebeisen S, Roller A, Czempinski K, Bertl A (2005) TPK1 is a vacuolar ion channel different from the slow-vacuolar cation channel 1. *Plant Physiol* 139:417–424. doi:10.1104/Pp.105.065599
13. Brohawn SG, Campbell EB, MacKinnon R (2013) Domain-swapped chain connectivity and gated membrane access in a Fab-mediated crystal of the human TRAAK K<sup>+</sup> channel. *Proc Natl Acad Sci U S A* 110:2129–2134. doi:10.1073/pnas.1218950110
14. Brohawn SG, del Mármol J, MacKinnon R (2012) Crystal structure of the human K2P TRAAK, a lipid- and mechano-sensitive K<sup>+</sup> ion channel. *Science* 335:436–441. doi:10.1126/science.1213808
15. Brohawn SG, Su Z, MacKinnon R (2014) Mechanosensitivity is mediated directly by the lipid membrane in TRAAK and TREK1 K<sup>+</sup> channels. *Proc Natl Acad Sci U S A* 111:3614–3619. doi:10.1073/Pnas.1320768111
16. Carraretto L, Formentin E, Teardo E, Checchetto V, Tomizioli M, Morosinotto T, Giacometti GM, Finazzi G, Szabó I (2013) A thylakoid-located two-pore K<sup>+</sup> channel controls photosynthetic light utilization in plants. *Science* 342:114–118. doi:10.1126/science.1242113
17. Chowdhury S, Jarecki BW, Chanda B (2014) A molecular framework for temperature-dependent gating of ion channels. *Cell* 158:1148–1158. doi:10.1016/j.cell.2014.07.026
18. Cid LP, Roa-Rojas HA, Niemeyer MI, González W, Araki M, Araki K, Sepúlveda FV (2013) TASK-2: a K2P K<sup>+</sup> channel with complex regulation and diverse physiological functions. *Front Physiol* 4:1–9. doi:10.3389/fphys.2013.00198
19. Cohen A, Ben-Abu Y, Hen S, Zilberberg N (2008) A novel mechanism for human K2P2.1 channel gating. Facilitation of C-type gating by protonation of extracellular histidine residues. *J Biol Chem* 283:19448–19455. doi:10.1074/jbc.M801273200
20. Derst C, Karschin A (1998) Evolutionary link between prokaryotic and eukaryotic K<sup>+</sup> channels. *J Exp Biol* 279:2791–2799. <http://jeb.biologists.org/content/201/20/2791.full.pdf+html>
21. Dunkel M, Latz A, Schumacher K, Müller T, Becker D, Hedrich R (2008) Targeting of vacuolar membrane localized members of the TPK channel family. *Mol Plant* 1:938–949. doi:10.1093/mp/ssn064
22. Enyedi P, Czirják G (2010) Molecular background of leak K<sup>+</sup> currents: two-pore domain potassium channels. *Physiol Rev* 90:559–605. doi:10.1152/physrev.00029.2009
23. Fritz-Laylin LK, Ginger ML, Walsh C, Dawson SC, Fulton C (2011) The *Naegleria* genome: a free-living microbial eukaryote lends unique insights into core eukaryotic cell biology. *Res Microbiol* 162:607–618. doi:10.1016/J.Resmic.2011.03.003
24. Fritz-Laylin LK, Prochnik SE, Ginger ML, Dacks JB, Carpenter ML, Field MC, Kuo A, Paredez A, Chapman J, Pham J, Shu S, Neupane R, Cipriano M, Mancuso J, Tu H, Salamov A, Lindquist E, Shapiro H, Lucas S, Grigoriev IV, Cande WZ, Fulton C, Rokhsar DS, Dawson SC (2010) The genome of *Naegleria gruberi* illuminates early eukaryotic versatility. *Cell* 140:631–642. doi:10.1016/j.cell.2010.01.032
25. Fromm J, Lautner S (2007) Electrical signals and their physiological significance in plants. *Plant Cell Environ* 30:249–257. doi:10.1111/j.1365-3040.2006.01614.x
26. Gajdanowicz P, Michard E, Sandmann M, Rocha M, Corrêa LGG, Ramírez-Aguilar SJ, Gomez-Porras JL, González W, Thibaud J-B, Van Dongen JT et al (2011) Potassium (K<sup>+</sup>) gradients serve as a mobile energy source in plant vascular tissues. *Proc Natl Acad Sci* 108:864–869. doi:10.1073/pnas.1009777108
27. Gilbert W (1985) Genes-in-pieces revisited. *Science* 228:823–824. doi:10.1126/science.4001923
28. Gobert A, Isayenkov S, Voelker C, Czempinski K, Maathuis FJM (2007) The two-pore channel TPK1 gene encodes the vacuolar K<sup>+</sup> conductance and plays a role in K<sup>+</sup> homeostasis. *Proc Natl Acad Sci U S A* 104:10726–10731. doi:10.1073/pnas.0702595104
29. Goldstein SAN (2011) K2P potassium channels, mysterious and paradoxically exciting. *Sci Signal* 4:pe35. doi:10.1073/pnas.0702595104
30. Goldstein SAN, Bayliss DA, Kim D, Lesage F, Plant LD (2005) International union of pharmacology. LV. Nomenclature and molecular relationships of two-P potassium channels. *Pharmacol Rev* 57:527–540. doi:10.1124/pr.57.4.12
31. González W, Riedelsberger J, Morales-Navarro SE, Caballero J, Alzate-Morales JH, González-Nilo FD, Dreyer I (2012) The pH sensor of the plant K<sup>+</sup>-uptake channel KAT1 is built from a sensory cloud rather than from single key amino acids. *Biochem J* 442:57–63. doi:10.1042/BJ20111498
32. González W, Zúñiga L, Cid LP, Arévalo B, Niemeyer MI, Sepúlveda FV (2013) An extracellular ion pathway plays a central role in the cooperative gating of a K(2P) K<sup>+</sup> channel by extracellular pH. *J Biol Chem* 288:5984–5991. doi:10.1074/jbc.M112.445528
33. Guex N, Peitsch MC (1997) SWISS-MODEL and the Swiss-Pdb Viewer: an environment for comparative protein modeling. *Electrophoresis* 18:2714–2723, PMID: 9504803
34. Hamamoto S, Marui J, Matsuoka K, Higashi K, Igarashi K, Nakagawa T, Kuroda T, Mori Y, Murata Y, Nakanishi Y, Maeshima M, Yabe I, Uozumi N (2008) Characterization of a tobacco TPK-type K<sup>+</sup> channel as a novel tonoplast K<sup>+</sup> channel using yeast tonoplasts. *J Biol Chem* 283:1911–1920. doi:10.1074/jbc.M708213200
35. Hedrich R (2012) Ion channels in plants. *Physiol Rev* 92:1777–1811. doi:10.1152/physrev.00038.2011
36. Hedrich R, Marten I (2011) TPC1-SV channels gain shape. *Mol Plant* 4:428–441. doi:10.1093/mp/ssr017



37. Honoré E (2007) The neuronal background K2P channels: focus on TREK1. *Nat Rev Neurosci* 8:251–261. doi:10.1038/nrn2117
38. Honoré E, Maingret F, Lazdunski M, Patel AJ (2002) An intracellular proton sensor commands lipid- and mechano-gating of the K(+) channel TREK-1. *EMBO J* 21:2968–2976. doi:10.1093/emboj/cdf288
39. Humphrey W, Dalke A, Schulten K (1996) VMD: visual molecular dynamics. *J Mol Graph* 14:33–38. doi:10.1016/0263-7855(96)00018-5
40. Hunter S, Jones P, Mitchell A, Apweiler R, Attwood TK, Bateman A, Bernard T, Binns D, Bork P, Burge S, de Castro E, Coghill P, Corbett M, Das U, Daugherty L, Duquenne L, Finn RD, Fraser M, Gough J, Haft D, Hulo N, Kahn D, Kelly E, Letunic I, Lonsdale D, Lopez R, Madera M, Maslen J, McAnulla C, McDowall J, McMenamin C, Mi H, Mutowo-Muellenet P, Mulder N, Natale D, Orengo C, Pesceat S, Punta M, Quinn AF, Rivoire C, Sangrador-Vegas A, Selengut JD, Sigrist CJ, Scheremetjew M, Tate J, Thimmajananathan M, Thomas PD, Wu CH, Yeats C, Yong S-Y (2012) InterPro in 2011: new developments in the family and domain prediction database. *Nucleic Acids Res* 40:D306–D312. doi:10.1093/nar/gkr948
41. Isayenkov S, Isner J, Maathuis FJM (2011) Membrane localization diversity of TPK channels physiological role. *Plant Signal Behav* 6: 1201–1204. doi:10.4161/psb.6.8.15808
42. Isayenkov S, Isner J-C, Maathuis FJM (2011) Rice two-pore K+ channels are expressed in different types of vacuoles. *Plant Cell* 23: 756–768. doi:10.1105/tpc.110.081463
43. Ketchum KA, Joiner WJ, Sellers AJ, Kaczmarek LK, Goldstein SAN (1995) A new family of outwardly rectifying potassium channel proteins with two pre domains in tandem. *Nature* 376:690–695. doi:10.1038/376690a0
44. Larkin MA, Blackshields G, Brown NP, Chenna R, McGettigan PA, McWilliam H, Valentin F, Wallace IM, Wilm A, Lopez R, Thompson JD, Gibson TJ, Higgins DG (2007) Clustal W and Clustal X version 2.0. *Bioinformatics* 23:2947–2948. doi:10.1093/bioinformatics/btm404
45. Lassmann T, Sonnhammer ELL (2005) Kalign—an accurate and fast multiple sequence alignment algorithm. *BMC Bioinforma* 6:298. doi: 10.1186/1471-2105-6-298
46. Latz A, Becker D, Hekman M, Müller T, Beyhl D, Marten I, Eing C, Fischer A, Dunkel M, Bertl A, Rapp UR, Hedrich R (2007) TPK1, a Ca(2+)-regulated Arabidopsis vacuole two-pore K(+) channel is activated by 14-3-3 proteins. *Plant J* 52:449–459. doi:10.1111/j. 1365-3113X.2007.03255.x
47. Latz A, Mehler M, Zapf S, Mueller TD, Wurzing B, Pfister B, Csaszar E, Hedrich R, Teige M, Becker D (2013) Salt stress triggers phosphorylation of the Arabidopsis vacuolar K+ channel TPK1 by calcium-dependent protein kinases (CDPKs). *Mol Plant* 6:1274–1289. doi:10.1093/mp/sss158
48. Lesage F, Guillemare E, Fink M, Duprat F, Lazdunski M, Romey G, Barhanin J (1996) TWIK-1, a ubiquitous human weakly inward rectifying K+ channel with a novel structure. *EMBO J* 15:1004–1011. doi:10.1073/pnas.1201132109
49. Maathuis FJM (2011) Vacuolar two-pore K+ channels act as vacuolar osmosensors. *New Phytol* 191:84–91. doi:10.1111/J.1469-8137. 2011.03664.X
50. Maingret F, Lauritzen I, Patel AJ, Heurteaux C, Reyes R, Lesage F, Lazdunski M, Honoré E (2000) TREK-1 is a heat-activated background K+ channel. *EMBO J* 19:2483–2491. doi:10.1093/emboj/19. 11.2483
51. Maîtrejean M, Wudick MM, Voelker C, Prinsi B, Mueller-Roeber B, Czempinski K, Pedrazzini E, Vitale A (2011) Assembly and sorting of the tonoplast potassium channel AtTPK1 and its turnover by internalization into the vacuole. *Plant Physiol* 156:1783–1796. doi: 10.1104/PP.111.177816
52. Marcel D, Müller T, Hedrich R, Geiger D (2010) K+ transport characteristics of the plasma membrane tandem-pore channel TPK4 and pore chimeras with its vacuolar homologs. *FEBS Lett* 584:2433–2439. doi:10.1016/j.febslet.2010.04.038
53. Mathie A (2007) Neuronal two-pore-domain potassium channels and their regulation by G protein-coupled receptors. *J Physiol* 578:377–385. doi:10.1113/jphysiol.2006.121582
54. Mathie A, Rees KA, El Hachmane MF, Veale EL (2010) Trafficking of neuronal two pore domain potassium channels. *Curr Neuropharmacol* 8:276–286. doi:10.2174/157015910792246146
55. Meyerowitz EM (2002) Plants compared to animals: the broadest comparative study of development. *Science* 295:1482–1485. doi:10. 1126/science.1066609
56. Miller AN, Long SB (2012) Crystal structure of the human two-pore domain potassium channel K2P1. *Sci* (80–) 335:432–436. doi:10. 1126/science.1213274
57. Mousavi SAR, Chauvin A, Pascaud F, Kellenberger S, Farmer EE (2013) Glutamate receptor-like genes mediate leaf-to-leaf wound signalling. *Nature* 500:422–426. doi:10.1038/nature12478
58. Niemeyer MI, González-Nilo FD, Zúñiga L, González W, Cid LP, Sepúlveda FV (2006) Gating of two-pore domain K+ channels by extracellular pH. *Biochem Soc Trans* 34:899–902. doi:10.1042/ BST0340899
59. Niemeyer MI, González-Nilo FD, Zúñiga L, González W, Cid LP, Sepúlveda FV (2007) Neutralization of a single arginine residue gates open a two-pore domain, alkali-activated K+ channel. *Proc Natl Acad Sci U S A* 104:666–671. doi:10.1073/pnas.0606173104
60. O'Kelly I, Butler MH, Zilberberg N, Goldstein SAN (2002) Forward transport. 14-3-3 binding overcomes retention in endoplasmic reticulum by dibasic signals. *Cell* 111:577–588. doi:10.1016/S0092-8674(02)01040-1
61. Patel AJ, Lazdunski M, Honoré E (2001) Lipid and mechano-gated 2P domain K(+) channels. *Curr Opin Cell Biol* 13:422–428. doi:10. 1016/S0166-2236(00)01810-5
62. Philippart K, Büchsenhütz K, Abshagen M, Fuchs I, Geiger D, Lacombe B, Hedrich R (2003) The K+ channel KZM1 mediates potassium uptake into the phloem and guard cells of the C4 grass *Zea mays*. *J Biol Chem* 278:16973–16981. doi:10.1074/jbc. M212720200
63. Piechotta PL, Rapedius M, Stansfeld PJ, Bollepalli MK, Ehrlich G, Ehrlich G, Andres-Enguix I, Fritzenschaft H, Decher N, Sansom MSP, Tucker SJ, Baukowitz T (2011) The pore structure and gating mechanism of K2P channels. *EMBO J* 30:3607–3619. doi:10.1038/emboj.2011.268
64. Rice P, Longden I, Bleasby A (2000) EMBOSS: Eur Mol Biol Open Softw Suite 16:2–3, PMID: 10827456
65. Sandoz G, Douguet D, Chatelain F, Lazdunski M, Lesage F (2009) Extracellular acidification exerts opposite actions on TREK1 and TREK2 potassium channels via a single conserved histidine residue. *Proc Natl Acad Sci U S A* 106:14628–14633. doi:10.1073/pnas. 0906267106
66. Schütze J, Krasko A, Custodio MR, Efremova SM, Müller IM, Müller WE (1999) Evolutionary relationships of Metazoa within the eukaryotes based on molecular data from Porifera. *Proc Biol Sci* 266:63–73. doi:10.1098/rspb.1999.0605
67. Sentenac H, Bonneaud N, Minet M, Lacroute F, Salmon J, Gaymard F, Grignon C (1992) Cloning and expression in yeast of a plant potassium ion transport system. *Science* 256:663–665. doi:10.1126/ science.1585180
68. Smart OS, Neduvilil JG, Wang X, Wallace BA, Sansom MSP (1996) HOLE: a program for the analysis of the pore dimensions of ion channel structural models. *J Mol Graph* 14:354–360. doi:10.1016/ S0263-7855(97)00009-X
69. Thiel G, Moroni A, Blanc G, Van Etten JL (2013) Potassium ion channels: could they have evolved from viruses? *Plant Physiol* 162: 1215–1224. doi:10.1104/pp. 113.219360
70. Troufflard S, Mullen W, Larson TR, Graham IA, Crozier A, Amtmann A, Armengaud P (2010) Potassium deficiency induces

- the biosynthesis of oxylipins and glucosinolates in *Arabidopsis thaliana*. *BMC Plant Biol* 10:172. doi:10.1186/1471-2229-10-172
71. Voelker C, Gomez-Porras JL, Becker D, Hamamoto S, Uozumi N, Gambale F, Mueller-Roeber B, Czempinski K, Dreyer I (2010) Roles of tandem-pore K<sup>+</sup> channels in plants—a puzzle still to be solved. *Plant Biol (Stuttg)* 56(Suppl 1):56–63. doi:10.1111/J.1438-8677.2010.00353.X
  72. Wang X, Zhang X, Dong X-P, Samie M, Li X, Cheng X, Goschka A, Shen D, Zhou Y, Harlow J, Zhu MX, Clapham DE, Ren D, Xu H (2012) TPC proteins are phosphoinositide-activated sodium-selective ion channels in endosomes and lysosomes. *Cell* 151:372–383. doi:10.1016/j.cell.2012.08.036
  73. Wu D, Hugenholtz P, Mavromatis K, Pukall R, Ivanova NN, Kunin V, Goodwin L, Wu M, Tindall BJ, Hooper SD, Pati A, Lykidis A, Spring S, Anderson IJ, Patrik D, Zemla A, Singer M, Lapidus A, Nolan M, Han C, Chen F, Cheng J, Lucas S, Kerfeld C, Lang E, Gronow S, Chain P, Bruce D, Rubin EM, Nikos C, Klenk H, Eisen JA (2009) A phylogeny-driven genomic encyclopaedia of Bacteria and Archaea. *Nature* 462:1056–1060. doi:10.1038/nature08656.A
  74. Zuzarte M, Heusser K, Renigunta V, Schlichthörl G, Rinné S, Wischmeyer E, Daut J, Schwappach B, Preisig-Müller R (2009) Intracellular traffic of the K<sup>+</sup> channels TASK-1 and TASK-3: role of N- and C-terminal sorting signals and interaction with 14-3-3 proteins. *J Physiol* 587:929–952. doi:10.1113/jphysiol.2008.164756
  75. Zuzarte M, Rinné S, Schlichthörl G, Schubert A, Daut J, Preisig-Müller R (2007) A di-acidic sequence motif enhances the surface expression of the potassium channel TASK-3. *Traffic* 8:1093–1100. doi:10.1111/j.1600-0854.2007.00593.x